Swelling of model polymer networks with different cross-link densities: A computer simulation study

Z.-Y. Lu and R. Hentschke*
Fachbereich Physik and Institute for Materials Science, Bergische Universität, D-42097 Wuppertal, Germany
(Received 24 June 2002; published 9 October 2002)

The swelling of model polymer networks with different cross-link densities is studied via molecular dynamics simulation. During the simulation, the solvent particles, consisting of one interaction center or six interaction centers, respectively, are transfered between two coupled simulation boxes. The gel box includes both network and solvent particles, whereas the solvent box contains solvent only. The particle transfer is controlled by the solvent chemical potential difference in the two boxes, which is calculated via the Widom test particle method for the one-site solvent and via Rosenbluth sampling for the chainlike solvent. The equilibrium swelling ratio of the network as well as the solvent diffusion coefficient under subcritical and supercritical conditions are computed as functions of the network cross-link density for a wide range of temperatures and pressures. In addition, the simulated swelling behavior is compared to a Flory-Huggins-type theory, which yields qualitative agreement for the systems studied here.

DOI: 10.1103/PhysRevE.66.041803 PACS number(s): 61.25.Hq, 05.10.−a, 05.50.+q, 05.20.−y

I. INTRODUCTION

A polymer network will swell or shrink by absorbing or expelling solvent molecules depending on the thermodynamic conditions. Because of this property, polymer networks are widely used in drug delivery, solvent selective absorption (separation), and other new technologies. Due to the complex structure of real polymer networks, it is difficult to relate the properties of a polymer network to its molecular structure via experimental methods. Here, molecular simulations can serve as ''computer experiments'' to elucidate this relation by unambiguously controlling the network structure. Usually the formation of networks, their topology and its consequences for processes like swelling is studied without including solvent explicitly in the simulations (e.g., Ref. [1]). Here, rather than focusing on the details of the formation of the network and the resulting physical properties, we focus on a structurally simple model network, but we include different solvents explicitly under controlled thermodynamic conditions.

Previously, Kenkare *et al.* have applied combined discontinuous molecular dynamics and Monte Carlo simulations to study the swelling of athermal polymer networks containing hard-sphere solvent [2]. In a grand canonical type ensemble, Escobedo and de Pablo have used the Monte Carlo method to discuss the swelling of athermal [3], square well, and modified Lennard-Jones polymer networks [4]. Using Gibbs-Ensemble molecular dynamics method [5,6], Aydt and Hentschke reported dynamic as well as structural results for swelling equilibria in model network-solvent systems using Lennard-Jones nonbonded interactions [7].

In two previous papers we have developed and applied a ''two-box-particle-transfer'' molecular dynamics simulation method to study the swelling behavior of model polymer networks under subcritical and supercritical conditions including solvent dynamics. In the first paper [8] the general algorithm was developed, and the method was used to study the swelling of a simple cubic network in contact with a one-site solvent. The results were compared to an extended Flory-Huggins model yielding good qualitative agreement. In the second paper [9] we investigated the swelling of a model network by a chainlike (six-site) solvent. Here the chains exhibit markedly different structural and dynamic properties in the corresponding gel and bulk phases due to the constraint imposed by the network.

In both references two coupled boxes, containing pure solvent and gel, respectively, will reach chemical equilibrium by exchanging solvent particles between them. The exchange is controlled by comparing the solvent chemical potentials measured continuously during a molecular dynamics simulation using either Widom's test particle method (for one-site solvents) [10] or Rosenbluth sampling (for chainlike solvents) [11]. In regular intervals a randomly selected solvent molecule is transfered instantaneously to reduce the so computed solvent chemical potential difference.

In this work we use the above method to study the effect of changing the network cross-link density both for the one-site and the chainlike or six-site solvent. The swelling ratios of the networks, which again have the simple cubic structure assumed previously, as well as the solvent diffusion coefficients under subcritical and supercritical conditions are computed. It is shown that networks with low cross-link density exhibit pronounced variation of the swelling ratio close to the critical point of the one-site solvent. The simulation results can be reproduced with very good qualitative accuracy using our modified Flory-Huggins theory developed in Ref. [8]. In comparison to the one-site solvent, the chainlike solvent results in a more complex swelling behavior. But again, the dependence of the swelling ratio on temperature and pressure becomes more pronounced as the cross-link density decreases. Similarly, the ratio D_N/D_S, diffusion coefficient of the solvent in the gel divided by the same quantity in the

*Author to whom correspondence should be addressed.

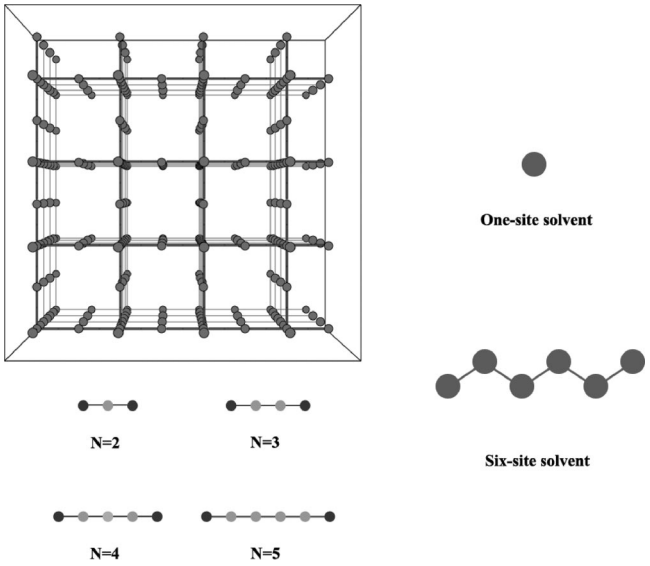

FIG. 1. Sketch of the model network and the two solvents. The number of bonds between two adjacent network cross links is denoted by N. The model network is shown with $N=2$.

bulk solvent at identical pressure and temperature, exhibits pronounced changes with pressure and temperature as the cross-link density decreases. Again, this is especially true for the one-site solvent close to its critical point.

II. SIMULATION METHOD AND MODEL CONSTRUCTION

The ''two-box–particle-transfer'' method was introduced in detail in Refs. [8,9]. During the simulations, one of the two boxes contains pure bulk solvent, whereas the other contains the model polymer network and the absorbed solvent. These two boxes will reach equilibrium by repeatedly exchanging solvent particles. Here the solvent particles are either one-site Lennard-Jones particles or six-site chains consisting of six sequentially bonded interaction centers. The solvent chemical potentials are calculated via Widom's test particle method or via Rosenbluth sampling, respectively. The calculation details are described in detail in Refs. [8,9].

For simplicity we adopt a perfect cubic model network that is similar to the used previously (cf. Fig. 1). The highest cross-link density corresponds to the model network with every second interaction center along the chain being a cross link. In this case we define $N=2$, where N denotes the number of bonds between two successive cross links. In the previous papers, we dealt with the extreme condition, i.e., the network has the highest cross-link density ($N=2$). In this paper, we will study the swelling behavior for $2 \leqslant N \leqslant 5$.

The potential energy $\mathcal{U}$ in each simulation box is given by $\mathcal{U}=\mathcal{U}_{LJ}+\mathcal{U}_{net}+\mathcal{U}_{val}$ [8,9]. $\mathcal{U}_{LJ}$ is the nonbonded Lennard-Jones potential energy. $\mathcal{U}_{net}$, which equals zero in the solvent box, is the interaction energy between bonded network beads. $\mathcal{U}_{val}$ is the intramolecular valence energy of the six-center solvent. $\mathcal{U}_{val}$ will be zero in the case of the one-center solvent, whereas for the six-center solvent $\mathcal{U}_{val}=u_{bond}+u_{bend}+u_{tors}$, i.e., we take the bond energy u_{bond}, the bond angle bending energy u_{bend}, and the torsion energy u_{tors} into account. All force field terms, their parameters, and the thermostat as well as the barostat coupling constants are compiled in Table I for the one-center solvent case and in Table II for the six-center solvent case, respectively. Note that here we have corrected typing errors in Table I of Ref. [8] and Table I of Ref. [9].

TABLE I. The force field parameters, and the thermostat, barostat parameters. The solvent possesses only one center of type C. N_N represents the network sites. Note that we have scaled the units such that $T_c^1=P_c^1=m^1=1$ in this table.

Lennard-Jones	σ	ϵ	m
C	0.457	0.779	1.0
N_N	0.580	0.779	1.0
Bond stretch	k_b	l_0	
N_N-N_N	9083.1	0.722	
	Value		
Δt	3.80×10^{-4}		
τ_T	3.80×10^{-2}		
τ_P/κ_T	8.52×10^{4}		

The equations of motion governing the time evolution in each individual simulation box are the same as in Ref. [8] [Eqs. (4)–(8)], i.e., we continue to use the weak coupling method due to Berendsen *et al.* [12]. The equations of motion are integrated via the leap-frog algorithm [13]. The solvent exchange between boxes, on the other hand, is governed by the following procedure. During the NPT simulation (i.e., particle number, pressure, and temperature are kept con-

TABLE II. The force field parameters, and the thermostat, barostat parameters. The six-center solvent is represented by $C_3-(C_2)_4-C_3$. N_N represents the network centers. Note that we have scaled the units such that $T_c^6=P_c^6=1$ in the six-center solvent case.

Lennard-Jones	σ	ϵ	m
C_2	0.2829	0.0902	1.0000
C_3	0.2980	0.1933	1.0713
N_N	0.3629	0.2924	1.1426
Bond stretch	k^b	l_0	
C_3-C_2	45239.10	0.1162	
C_2-C_2	45239.10	0.1162	
N_N-N_N	8699.83	0.4526	
Angle bend	k^θ [rad^{-2}]	θ_0 [°]	
$C_3-C_2-C_2$	123.11	114.0	
$C_2-C_2-C_2$	123.11	114.0	
Torsion	c_1	c_2	c_3
$X-C_2-C_2-X$	0.6988	−0.1338	1.5582
Parameter	Value		
Δt	4.14×10^{-4}		
τ_T	4.14×10^{-2}		
τ_P/κ_T	9.28×10^{4}		

TABLE III. The initial numbers of particles in each simulation box. $N^{(N)}$ represents the number of network beads. $N_S^{(N)}$ is the number of solvent particles in the network box, and $N_S^{(S)}$ is the number of solvent particles in the solvent box.

	$N=3$	$N=4$	$N=5$
One-site solvent	$N^{(N)}=448$ $N_S^{(N)}=192$ $N_S^{(S)}=1000$	$N^{(N)}=270$ $N_S^{(N)}=130$ $N_S^{(S)}=2067$	$N^{(N)}=351$ $N_S^{(N)}=149$ $N_S^{(S)}=2500$
Six-site solvent	$N^{(N)}=448$ $N_S^{(N)}=36$ $N_S^{(S)}=180$	$N^{(N)}=270$ $N_S^{(N)}=36$ $N_S^{(S)}=180$	$N^{(N)}=351$ $N_S^{(N)}=36$ $N_S^{(S)}=180$

stant), the solvent chemical potentials in the two simulation boxes are calculated continuously via the Widom's test particle method for the one-site solvent or via the Rosenbluth sampling method for the six-site solvent. In the former case 5×10^4 test particles will be randomly generated during 2×10^3 time steps to obtain the solvent chemical potential. In the latter case the excess solvent chemical potential is computed from averages based on 1.2×10^4 trial chains constructed during 4×10^3 time steps at randomly selected locations in each box. The solvent exchange between the two simulation boxes is controlled by direct comparison of the so computed solvent chemical potentials. Each solvent particle is associated with a transfer variable ξ, which is equal to 0 or 1 depending on whether the solvent particle resides in the network box or in the solvent box. This means that all terms in the expression for the total energy involving solvent particle i are multiplied by ξ_i in one box and by $1-\xi_i$ in the other. A solvent particle is transfered by changing its ξ value from 0 to 1 or from 1 to 0 attempting to reduce the chemical potential difference. This transfer is instantaneous, i.e., a randomly selected solvent particle in one box will be forced into the other box.

Initially we start the simulation with $N^{(N)}$ nontransferable network beads and $N_S^{(N)}$ solvent particles distributed homogeneously in box 0, whereas box 1 contains $N_S^{(S)}$ solvent particles (cf. Table III). To relax the unfavorable initial network geometry, a 10^5 time step-NVT simulation is executed without solvent transfer. Subsequently, the NPT simulation is carried out allowing solvent exchange. Typical simulation runs range from 3×10^6 to 6×10^6 time steps for the one-site solvent and from 1×10^6 to 2×10^6 time steps for the six-site solvent.

III. RESULTS AND DISCUSSION

In the following we scale the simulation temperatures and pressures by the corresponding critical values of the one-site solvent (T_c^1, P_c^1) and the six-site solvent (T_c^6, P_c^6), respectively. For the one-site solvent, $T_r=T/T_c^1$ takes on the values 0.89, 1.05, and 2.10, and $P_r=P/P_c^1$ takes on the values 1.30, 2.17, 4.34, 6.52, 8.69, 10.86, 13.02, and 15.20. For the six-site solvent, $T_r=T/T_c^6$ takes on the values 0.89, 1.05, 1.26, and 1.64, and $P_r=P/P_c^6$ takes on the values 2.17, 4.34, 6.52, 8.69, and 10.86.

For the one-site solvent, Fig. 2(a) shows the network swelling ratios q at different cross-link densities ($N=5$, $N=4$, $N=3$, and $N=2$). Note the q is defined as the ratio $V(T,P)/V_0(T,P)$, where V is the volume of the swollen network, and V_0 is the value of the dry network. The data for $N=2$ are taken from Ref. [8] and shown for comparison. At the subcritical temperature $T_r=0.89$, all networks shrink rapidly with increasing pressure. For $P_r>2.0$, however, q is virtually independent of P. Note also that in this range networks with low cross-link density show significantly larger q values, i.e., $q(N=5)$ is about three times larger then $q(N$

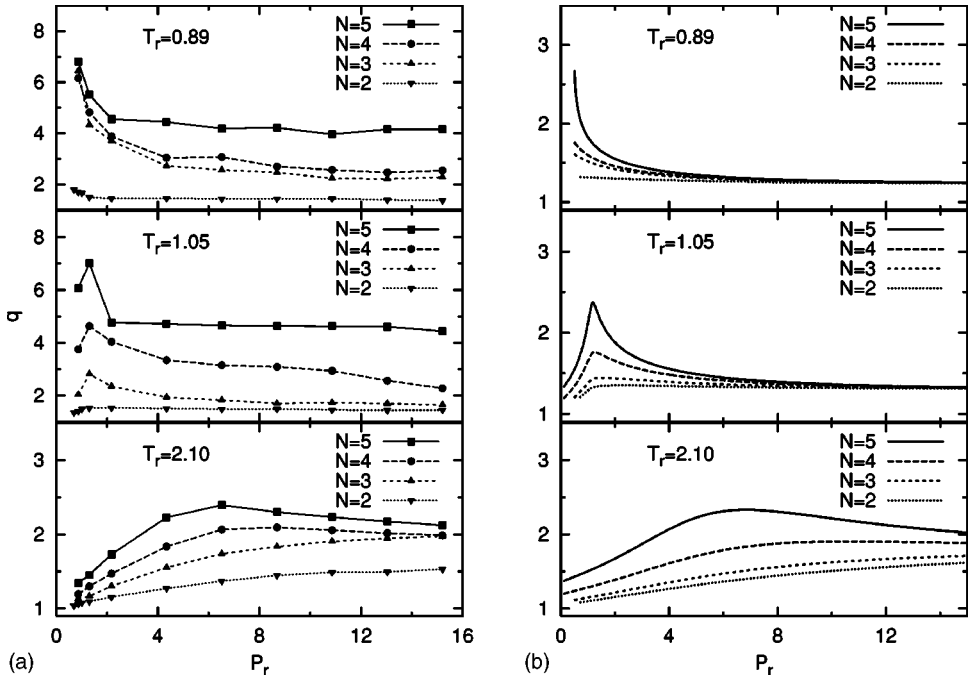

FIG. 2. (a) Swelling ratio q vs reduced pressure P_r for the one-site solvent. $T_r=0.89$, 1.05, and 2.10. The symbols represent simulation results, and the lines serve to guide the eye. (b) Corresponding results of the modified Flory-Huggins theory. $\chi_1=2.0/T_r$, $\chi=0.7/T_r+0.5$, and $\chi_2=0.2/T_r+2.2$ for $N=2$, $\chi_2=0.2/T_r+1.45$ for $N=3$, $\chi_2=0.2/T_r+1.3$ for $N=4$, and $\chi_2=0.2/T_r+1.0$ for $N=5$.

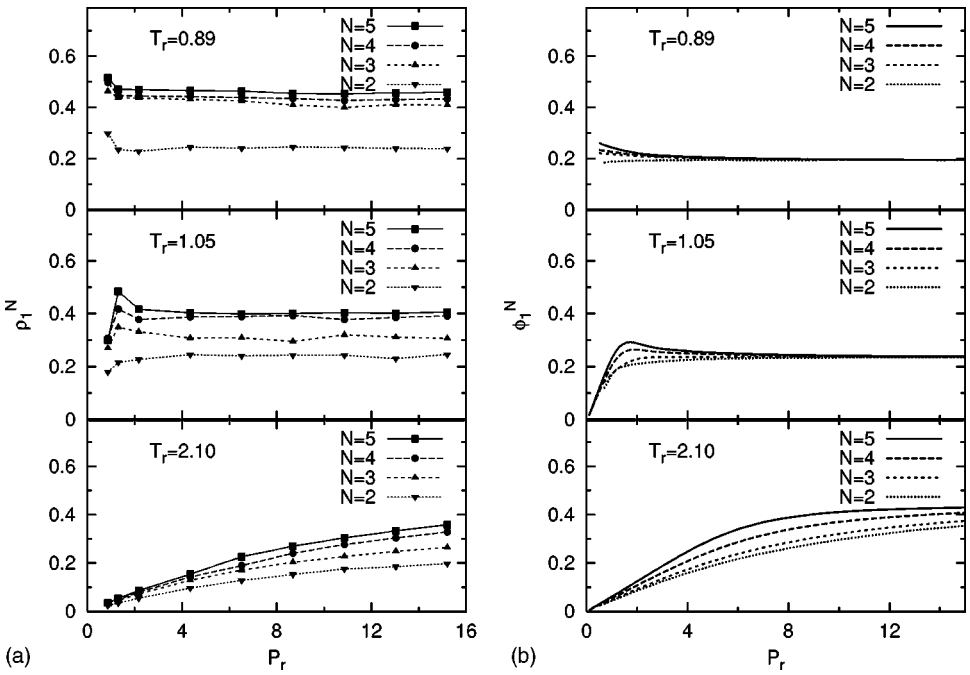

FIG. 3. (a) Solvent number density in the gel ρ_1^N vs P_r for the one-site solvent. $T_r=0.89$, 1.05, and 2.10. The symbols represent simulation results, and the lines serve to guide the eye. (b) Corresponding results of the modified Flory-Huggins theory. Here ϕ_1^N is the solvent volume fraction in the gel.

$=2$). From a thermodynamic point of view, this is mainly due to the competition between the network elasticity and the solvent osmotic pressure. Solvent particles will be ''pressed'' from their bulk phase into the dry network in order to decrease the solvent chemical potential difference between them (which is the origin of osmotic pressure), and the network swells. On the contrary, the configuration entropy of the network decreases due to the swelling. It is clear that for lower cross-link densities, the network can swell more strongly before the elastic reaction becomes pronounced enough to counteract the solvent's osmotic pressure [3]. At $T_r=1.05$, a temperature near the critical value, all networks independent of their cross-link densities exhibit a peak in the swelling isotherms around $P_r=2.0$. Above $P_r=2.0$ the swelling ratio q again varies little as the pressure increases. Note that this obvious peak has not been reported by other researchers. In Ref. [8] it is attributed to the competing effects of the excess chemical potential and the density ratio as functions of pressure. In addition, networks with different cross-link densities still show the strong increase of q with increasing N at constant P. For example, at large P, the swelling ratio $q(N=5)$ is about three times larger than $q(N=2)$. Finally, the bottom panel in Fig. 2(a) shows q vs P at $T_r=2.10$ for different cross-link densities. For high cross-link densities ($N=2$ and $N=3$), the networks swell monotonically with increasing pressure, whereas the swelling curves for low cross-link density networks show apparent peaks between $P_r=6.0$ and $P_r=8.0$. Again, networks with higher cross-link density swell more strongly than those with lower cross-link density, although the difference between swelling ratios is not as pronounced as for the two other temperatures. We note that the reduction of the swelling ratio with increasing network cross-link density is in agreement with the reports in Refs. [2,3] for athermal gels.

Figure 2(b) shows the corresponding isotherms for the one-site solvent obtained from our modified Flory-Huggins model [8], which includes empty lattice sites, to make the system compressible. This model contains three site-site interaction parameters ($\chi=-q_z(\epsilon_{11}+\epsilon_{22}-2\epsilon_{12})/(2k_BT)$, $\chi_1=-q_z\epsilon_{11}/(2k_BT)$, and $\chi_2=-q_z\epsilon_{22}/(2k_BT)$; q_z is the lattice coordination, and ϵ_{11}, ϵ_{22}, and ϵ_{12} are site-site interaction energies, where 1 indicates solvent and 2 indicates network sites). The interaction parameter χ_1 is obtained from the critical isotherm of the one-site solvent (cf. Ref. [8]). The other two parameters, χ and χ_2, are written as $\chi=uT_c^1/T+v$ and $\chi_2=u_2T_c^1/T+v_2$. u, v, u_2, and v_2 are adjusted to semiquantatively reproduce the simulation results obtained at $T_r=2.10$. At the other two temperatures, $T_r=0.89$ and $T_r=1.05$, the results of the modified Flory-Huggins model qualitatively agree with the simulation results. Note that the characteristic swelling behavior, i.e., at $T_r=0.89$ the networks shrink sharply with increasing pressure below $P_r=2.0$, and at $T_r=1.05$ the swelling curves show peaks below $P_r=2.0$, is reproduced by the modified Flory-Huggins model. Notice also that with increasing cross-link density the network swelling ratio decreases at a constant pressure. However, the decrease, at least close to $T_r=1.0$, is much less in the simulation. Because this is a mean-field model which neglects correlation effects, we may attribute this strong N dependence at large pressure to structural correlations.

Figure 3 shows the number density of solvent in the gel, ρ_1^N, obtained from the simulations and the corresponding solvent volume fraction in the gel, ϕ_1^N, obtained from our modified Flory-Huggins theory. Again the theory reproduces the simulations qualitatively, i.e., the densities exhibit the same shape as the corresponding swelling curves [cf. Fig. 2(a)] under the same conditions. As in the case of q we

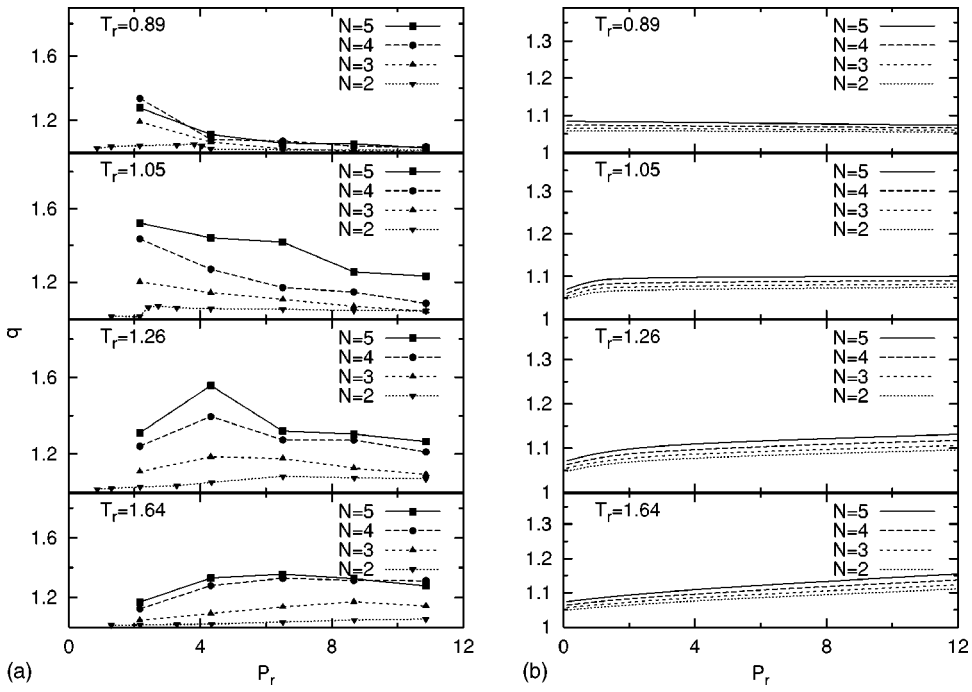

FIG. 4. (a) Swelling ratio q vs P_r for the six-site solvent. $T_r=0.89$, 1.05, 1.26, and 1.64. The symbols represent simulation results, and the lines serve to guide the eye. (b) Corresponding results of the modified Flory-Huggins theory. $\chi_1=0.992/T_r$, $\chi=0.7/T_r-0.3$, and $\chi_2=0.3/T_r+1.1$ for $N=2$, $\chi_2=0.3/T_r+1.0$ for $N=3$, $\chi_2=0.3/T_r+0.9$ for $N=4$, and $\chi_2=0.3/T_r+0.8$ for $N=5$.

observe that close to T_c and at high pressure the theoretical curves for different N converge, a consequence of the neglect of structural correlations. Note that the same parameters are used in both Figs. 2 and 3. It is also shown in Fig. 3(a) that networks with lower cross-link density can uphold more solvent particles. Notice, however, that the relative increase of ρ_1^N close to T_c becomes less as N increases, whereas the reverse is true for q in Fig. 2(a).

Figure 4(a) shows the swelling curves of model networks with different cross-link densities in the case of the six-site solvent (the data for $N=2$ are taken from Ref. [9]). Comparing Fig. 4(a) with Fig. 2(a) we observe that the overall magnitude of the swelling ratio q is greatly reduced for the chainlike solvent. For lower cross-link densities ($N=5$, $N=4$, and $N=3$) the networks shrink with increasing pressure at $T_r=0.89$ and at $T_r=1.05$. This is similar to the swelling behavior of the same networks in contact with one-site solvent at $T_r=0.89$. However, the isotherms for cross-link density $N=2$ show peaks at these two temperatures, which is qualitatively similar to the swelling curves obtained for the one-site solvent at $T_r=1.05$. At $T_r=1.26$, all swelling ratios increase with increasing pressure, reach a maximum, and subsequently decrease. This is similar to the behavior in the case of the one-site solvent as T_r approaches one. The $T_r=1.64$ curves show broad maxima for networks with lower cross-link densities, whereas for $N=2$, q increases monotonously with increasing pressure (with an apparent maximum at higher P_r). Again this behavior is qualitatively similar to the swelling behavior obtained for the one-site solvent at high T_r. Comparing the q values of different networks in Fig. 4(a), we find that by increasing the cross-link density, the swelling ratio overall is greatly decreased at the same T_r. This reflects the constraining effect of the network with higher cross-link density on the swelling behavior, which is the same as in one-site solvent case.

Figure 4(b), in analogy to Fig. 2(b), shows the corresponding isotherms for the chainlike solvent obtained from the modified Flory-Huggins model. Here the interaction parameters are obtained as follows. The solvent-solvent and the solvent-network interaction parameters, which are all identical for all curves shown here, are taken from Ref. [9]. The network-network interaction parameter decreases with decreasing cross-link density. Whereas simulation and theory show close accord in Fig. 2, for the chainlike solvent we find rough qualitative agreement only. Note that the order of the curves for each temperature is the same. In addition, both simulation and theory yield isotherms with overall negative slope at $T_r=0.89$ and isotherms with overall positive slope at $T_r=1.64$. However, the crossover between these behaviors apparently occurs at a lower temperature, and there are no explicit maxima in the theoretical curves.

Changing the network cross-link density not only varies the network swelling behavior, but also produces pronounced effects on the solvent dynamics. In contrast to pure Monte Carlo methods, our algorithm allows to study the dynamics of the solvent inside the networks. E.g., we can obtain the solvent center of mass self-diffusion coefficient via the Einstein relation [13],

$$D=\lim_{t\to\infty}\langle|\vec{r}_i(t)-\vec{r}_i(0)|^2\rangle/6t, \tag{1}$$

where $\vec{r}_i(t)$ is the position of molecule i at time t. For the same simulations as in Fig. 2(a) the ratio D_N^1/D_S^1 vs P_r is shown in Fig. 5. Here D_N^1 is the self-diffusion coefficient of the one-site solvent in the gel, and D_S^1 is the corresponding

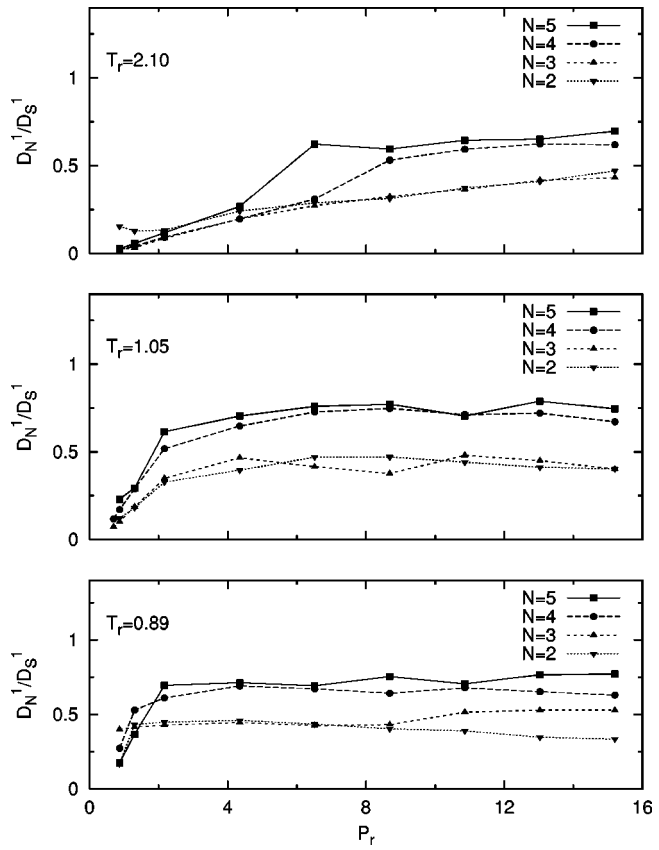

FIG. 5. The ratio of the one-site solvent self-diffusion coefficients in the network and in the bulk D_N^1/D_S^1 as function of reduced pressure P_r. The symbols are the simulation results, whereas the lines serve to guide the eye.

quantity in the bulk one-site solvent. At $T_r=2.10$, the highest temperature considered here, D_N^1/D_S^1 shows an overall increase with increasing pressure. At the other two temperatures, i.e., $T_r=0.89$ and $T_r=1.05$, the ratio D_N^1/D_S^1 exhibits flat maxima for $N=2$, whereas for networks with lower cross-link densities D_N^1/D_S^1 increases sharply below $P_r \approx 4$, but remains virtually constant at large P. Moreover, it is shown in Fig. 5 that with increasing cross-link density, the ratio D_N^1/D_S^1 reduces accordingly.

Figure 6 shows the ratio D_N^6/D_S^6 vs P_r for the different networks. These results are for the simulations discussed in Fig. 4. Here D_N^6 is the self-diffusion coefficient of the six-site solvent in the gel, and D_S^6 is the corresponding quantity in bulk six-site solvent. At $T_r=1.64$, the highest temperature, the ratio D_N^6/D_S^6 increases monotonously with increasing pressure for all networks. At the lowest temperature here, $T_r=0.89$, the high temperature behavior is reversed, i.e., D_N^6/D_S^6 decreases for all networks except for the $N=2$ network, for which D_N^6/D_S^6 still increases monotonously. For the intermediate temperatures, $T_r=1.26$ and $T_r=1.05$, we observe the crossover between the above behaviors, i.e., a maximum appears in the curve for $N=3$ at $T_r=1.26$ and subsequently also for $N=4,5$ at $T_r=1.05$. In general the ratio D_N^6/D_S^6 decreases with increasing network cross-link density.

Assuming Arrhenius behavior, i.e., $D=D^{(0)}\exp(-E/k_BT)$, we calculate the activation energy E of the six-site solvent self-diffusion and the corresponding pre-exponential factor $D^{(0)}$ [9]. Figure 7(a) shows the activation energies for solvent diffusion in the network, E_N, divided by the same quantity in the bulk, E_S, vs reduced pressure for different

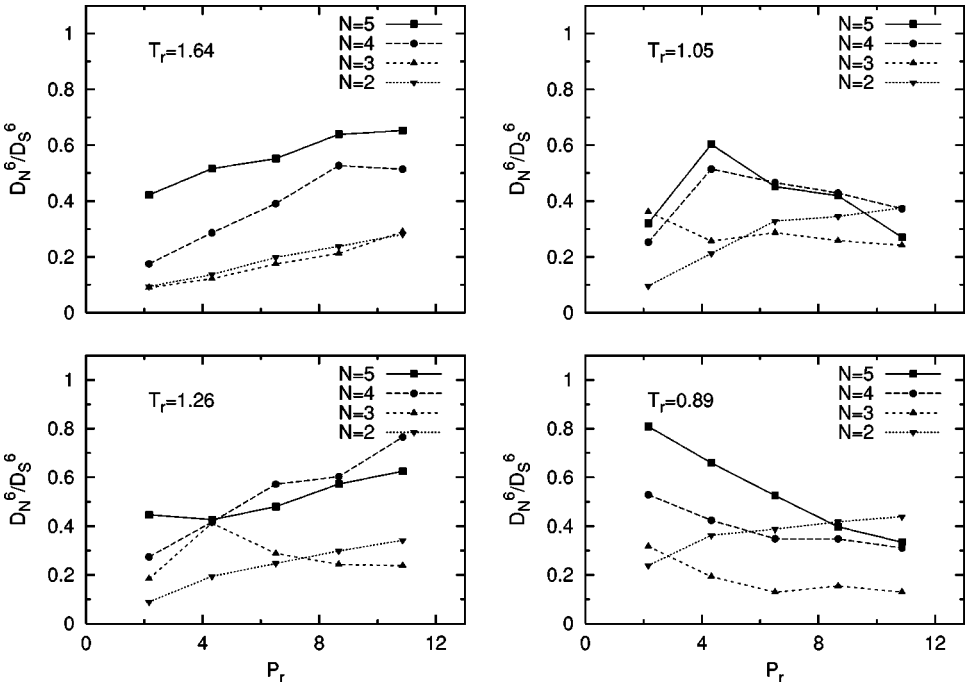

FIG. 6. The ratio of the six-site solvent self-diffusion coefficients in the network and in the bulk D_N^6/D_S^6 as a function of reduced pressure P_r. The symbols are the simulation results, whereas the lines serve to guide the eye.

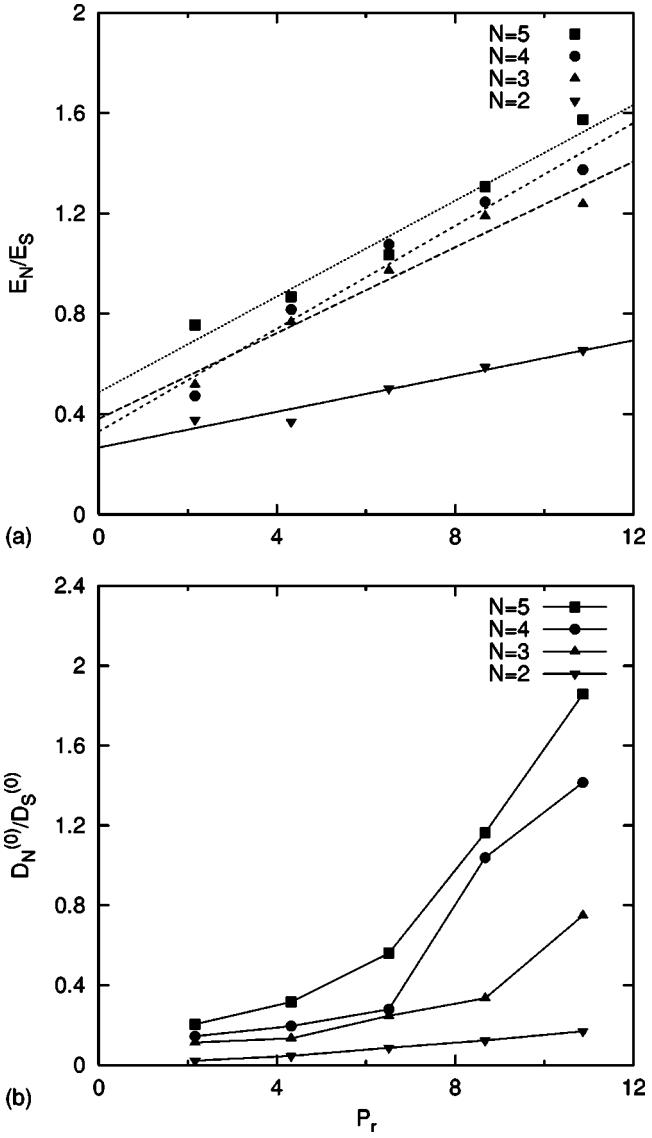

FIG. 7. (a) Activation energies for solvent diffusion inside the network E_N divided by the same quantity in the bulk solvent E_S vs reduced pressure. Solid line, straight line fits to the data for $N=2$; long dashes, fit to $N=3$; shot dashes, fit to $N=4$; dots, fit to $N=5$. This figure is based on Fig. 6. (b) Ratio of the preexponential factors vs reduced pressure. The lines serve to guide the eye.

network cross-link densities. For each cross-link density E_N/E_S increases close to linearly with increasing pressure. Furthermore, E_N/E_S increases with decreasing cross-link density in general (Obviously, for $N\rightarrow\infty$ this trend cannot continue, because E_N/E_S should approach unity). In the case of $N=2$, E_N/E_S has a smaller slope, and the values are overall smaller than unity, whereas in the cases of lower cross-link densities, E_N/E_S is larger than unity at high pressure. Figure 7(b) shows the corresponding ratio of the preexponential factors vs P_r for the different N. $D_N^{(0)}/D_S^{(0)}$ increases with increasing pressure and decreasing cross-link density. In the cases of high cross-link density ($N=2$ and $N=3$) $D_N^{(0)}/D_S^{(0)}$ is overall smaller than unity, whereas in the cases of low cross-link density ($N=4$ and $N=5$) $D_N^{(0)}/D_S^{(0)}$ is larger than unity at high pressure. Previously, in the case of $N=2$, we have attributed the hindrance effects of the network on the solvent mobility to the small number of suitable holes (corresponding to small $D^{(0)}$ values) permitting a solvent molecule to move [9]. This interpretation appears to be valid for the other cross-link densities also if the pressure is low. However, $D_N^{(0)}/D_S^{(0)}$ and E_N/E_S both may exceed unity at high pressure (at least for $N=4,5$). In these cases, the solvent diffusion behavior in the network is different. It is not mainly controlled by the available holes for the solvent molecules in the network, but the activation energy, which now is larger in the network, dominates the behavior.

IV. CONCLUSION

In a series of papers we have investigated the swelling of model polymer networks using both computer simulations and a lattice theory. In Ref. [8], a two-box–particle-transfer method was developed and applied to study the swelling of a strongly cross-linked network in contact with explicit one-site solvent. In addition, we modified the Flory-Huggins theory by including empty sites to obtain the swelling isotherms of the networks. This theory yielded excellent qualitative agreement with the simulation. In Ref. [9], the simulation method was extended to include chainlike solvent, and in particular, the method for measuring the solvent chemical potential was modified.

Here, in a concluding paper, we study the swelling of networks with different cross-link densities in contact with one-site and chainlike solvents. The equilibrium swelling ratio of the network as well as the solvent diffusion coefficient under subcritical and supercritical conditions are computed as functions of the network cross-link density for a wide range of temperatures and pressures. For the swelling isotherms of the one-site solvent we find excellent qualitative agreement between simulation and theory for all cross-link densities. In the case of the chainlike solvent we only find partial qualitative agreement.

ACKNOWLEDGMENT

One of the authors (Z.Y.L.) thanks Enno Oyen for checking the parameters in Table I and Table II.

[1] S. Lay, J.-U. Sommer, and A. Blumen, J. Chem. Phys. **110**, 12173 (1999); **113**, 11355 (2000), and references therein.

[2] N.R. Kenkare, C.K. Hall, and S.A. Khan, J. Chem. Phys. **113**, 404 (2000).

[3] F.A. Escobedo and J.J. de Pablo, J. Chem. Phys. **106**, 793 (1997).

[4] F.A. Escobedo and J.J. de Pablo, J. Chem. Phys. **110**, 1290 (1999).

[5] M.J. Kotelyanskii and R. Hentschke, Phys. Rev. E **51**, 5116 (1995).
[6] M.J. Kotelyanskii and R. Hentschke, Mol. Simul. **17**, 95 (1996).
[7] E.M. Aydt and R. Hentschke, J. Chem. Phys. **112**, 5480 (2000).
[8] Z.-Y. Lu and R. Hentschke, Phys. Rev. E **63**, 051801 (2001).
[9] Z.-Y. Lu and R. Hentschke, Phys. Rev. E **65**, 041807 (2002).
[10] B. Widom, J. Chem. Phys. **39**, 2802 (1963).
[11] M.N. Rosenbluth and A.W. Rosenbluth, J. Chem. Phys. **23**, 356 (1955).
[12] H.J.C. Berendsen, J.P.M. Postma, W.F. van Gunsteren, A. DiNola, and J.R. Haak, J. Chem. Phys. **81**, 3684 (1984).
[13] M.P. Allen and D.J. Tildesley, *Computer Simulations of Liquids* (Oxford Science, Oxford, 1987).